

# Electronic band structure of novel 18-K superconductor $Y_2C_3$ as compared with YC and $YC_2$ .

I.R. Shein\* and A.L. Ivanovskii

*Institute of Solid State Chemistry, Ural Branch of the Russian Academy of Sciences, 620219, Ekaterinburg, Russia*

The electronic band structure of yttrium sesquicarbide  $Y_2C_3$  ( $Pu_2C_3$  structural type) reported by Akimitsu et al. (2003) as a novel 18-K superconductor is investigated using the first-principle full-potential LMTO method and compared with those of yttrium mono- and dicarbide: cubic YC and 4-K superconductor  $YC_2$  ( $CaC_2$  structural type). Our results show that the enhanced  $T_c$  of  $Y_2C_3$  as compared with  $YC_2$  may be interpreted by the electronic factors: the near-Fermi DOS for  $Y_2C_3$  was found to be about 70 % higher than for  $YC_2$ , and the contribution from the C2p states increases. The Fermi level of the "ideal" stoichiometric bcc  $Y_2C_3$  is located near the local DOS minimum, and the superconducting properties of  $Y_2C_3$ -based materials would be very sensitive to synthesis conditions and the presence of impurities and lattice vacancies. We suppose that by changing these factors it is possible to vary  $T_c$  for the yttrium sesquicarbide.

\* E-mail: shein@ihim.uran.ru

PACS numbers: 74.70.-b, 71.20.-b

## I. Introduction.

Metal carbides represent a technologically important group of materials with interesting properties including extreme hardness, high melting temperatures, and superconductivity<sup>1</sup>.

Among superconducting binary compounds, metal carbides are known as conventional low-temperature BCS superconductors (SC) and have long been examined<sup>2</sup>. Comparison of different classes of binary carbides: semi- ( $M_2C$ ), mono- (MC), sesqui- ( $M_2C_3$ ), and dicarbides ( $MC_2$ ) shows (reviews<sup>2,3</sup>) that the majority of the known superconductors are found among cubic compounds with a rock-salt structure (B1), in which C and M atoms are in octahedral surrounding. Among these phases, the maximum values of transition temperatures  $T_c$  belong to Ta (10.2), W (10 K), Nb (11.1), and Mo (14.3 K) monocarbides<sup>3</sup>. Using the first-principle band structure calculations results, it was proposed that B1-MoC (isoelectronic and isostructural to the 16.6-K superconductor NbN<sup>3</sup>) was the prime candidate for the "highest-temperature" SC among all familiar metal carbides with a predicted transition temperature of about 20 K<sup>4</sup>.

The superconducting state is much less pronounced for the dicarbides, in which C atoms are in the form of isolated  $C_2$  pairs. Among metal dicarbides, the low-temperature SC was observed only for three compounds  $MC_2$  ( $M = Y, La, Lu$ ) with the highest  $T_c$  value of 3.9 K for  $YC_2$ <sup>3</sup>. In addition, some superconducting metal sesquicarbides have been also described, for example several compounds with  $T_c$  of about 11 K ( $La_2C_{2.7}$  and  $Y_2C_3$ ) and 15 K ( $Lu_2C_3$ )<sup>3</sup>.

The interest in the properties of the yttrium carbide systems increased in the past years due to the discovery of superconductivity with transition temperatures up to 11.6 K in the layered yttrium carbide halides  $Y_2C_2I_2$  ( $T_c = 9.97$  K) and  $Y_2C_2Br_2$  ( $T_c = 5.04$  K)<sup>5</sup> and

also because of the observation of superconductivity with  $T_c \sim 15-23$  K<sup>6,7</sup> in more complex systems: Y-Ni and Y-Pd-based borocarbides, see also reviews<sup>8,9,10</sup>. In this context, binary and quasi-binary Y carbides (especially Th-doped yttrium dicarbide  $(Y_{1-x}Th_x)C_2$ <sup>13</sup>) also attracted particular attention since their  $T_c$  values are close to those of A15 compounds<sup>2,3</sup>.

Quite recently, Akimitsu et al<sup>12</sup> have carried out a high-pressure synthesis of a novel superconducting phase in the Y-C system with  $T_c$  of about 18 K and assumed that this 18-K SC originated in the yttrium sesquicarbide  $Y_2C_3$  with the body-centered cubic (bcc)  $Pu_2C_3$ -type crystal structure.

The value of  $T_c$  for  $Y_2C_3$  obtained in magnetic measurements<sup>14</sup> was reported earlier to be 11 K. It was pointed out<sup>13</sup> that the superconductivity in the Y-C yttrium system is very sensitive to the synthesis conditions, for instance pressure and heat treatment. In particular, the effect of carbon nonstoichiometry was observed. In Ref.<sup>14</sup>, the bcc  $Y_2C_3$  has been synthesized by arc-melting and high-pressure techniques. Magnetic susceptibility showed that the material exhibited superconductivity with variable  $T_c$  ranging from 6 K to 11.5 K. In Ref.<sup>12</sup>, the superconducting  $Y_2C_3$  phase was prepared under high pressure using mixed powders (Y+C) in a BN cell. It is noteworthy that the lattice parameter (a) changes for different sintering processes and exists in the range between 0.8181 and 0.8226 nm<sup>12</sup> as distinct from earlier findings (0.8214 - 0.8251 nm)<sup>13</sup>. One of the reasons may be the difference in the pressure range (4-5.5<sup>12</sup> compared with 1.5-2.5 GPa<sup>13</sup>). Furthermore, the authors<sup>14</sup> successfully reproduced the result<sup>12</sup> and reported the synthesis of the 18-K phase with some differences in the experimental technique. In addition, a sample with the nominal composition  $Y_2C_{2.9}B_{0.1}$  was prepared to check a possible role of boron impurities from the BN cell used in the experiments<sup>12</sup>. According to data<sup>14</sup>, the 18-K phase coexists with another phase

(the 11-K phase reported in<sup>13</sup>) having a trace of a low- $T_c$  phase (4 K). This "impurity" phase is  $YC_2$ . Moreover, the  $T_c$  for the boron-doped sample (16.4 K) is lower than that of the "pure" carbide. This means that boron impurities in the C positions play a negative role in the Y-C superconductivity. It was also reported that the magnetization (M-H) curves of the 18-K  $Y_2C_3$  phase showed a type-II superconducting behavior<sup>12</sup>. While an explanation for the observed<sup>12,14</sup> behavior in the 18-K material based on a microscopic theory is still lacking, it is necessary to perform comparative studies of the electronic properties of yttrium carbide phases. In this paper, we report the theoretical results related to the electronic band structure of bcc  $Y_2C_3$  in comparison with other yttrium carbide phases, namely the B1 monocarbide YC and 4-K SC  $YC_2$ . The electronic bands, density of states (DOS) and site-projected l-decomposed DOS near the Fermi energy ( $E_F$ ) of these carbides are obtained and analyzed as a function of structures and nominal stoichiometry: YC ( $C/Y=1$ ) >  $Y_2C_3$  ( $C/Y=1.5$ ) >  $YC_2$  ( $C/Y=2$ ).

## II. Models and Method of Calculation.

The yttrium carbides have cubic (YC,  $Y_2C_3$ ) and tetragonal ( $YC_2$  - space group I4/mmm) crystal structures. The yttrium sesquicarbide crystallizes in a bcc structure of the  $Pu_2O_3$  type (space group I-43d) with the lattice parameter  $a = 0.8233$  nm (ICSD-CC No.86290) and eight formula units per a unit cell<sup>15</sup>. The Wyckoff positions for atoms are Y:16c (0.05;0.05;0.05) and C:24d (0.2821;0;1/4). The band structure of the above-mentioned carbides was calculated using the scalar relativistic full-potential linear muffin-tin method (FLMTO)<sup>16</sup> with using the generalized gradient approximation (GGA) of Perdew et al.<sup>17</sup>. The  $Y_2C_3$  structural parameters are taken from Ref.<sup>15</sup>. The calculated equilibrium values of lattice constants obtained from minimum total energy and are  $a = 0.5076$  nm for YC and  $a = 3.699$  nm,  $c = 6.140$  nm,  $x = 0.37478$  for  $YC_2$ .

## III. Results.

In Fig. 1 we show our FLMTO band structure of B1-YC. The YC band structure is very similar to that found for other rock-salt (B1) transition metal carbides, see for example<sup>4,18,19,20</sup>, consist from low-energy C2s band, does not contribute to the bonding. This band exhibits the maximum dispersion (2.35 eV) between  $\Gamma$  and L points. The next bands separated from the C2s band by a gap at about 3.34 eV originate mainly from mixed C2p-Y4d states. The Y4d bands are decomposed into  $e_g$  and  $t_{2g}$  components with energies 1.82 and 3.49 eV in  $\Gamma$  point above the Fermi level ( $E_F$ ). In B1 carbides, the  $e_g$ -like bands mixed with the C2p states are usually viewed as the bonding part of the d-p hybridization zone, while  $t_{2g}$  - as the antibonding part overlapping the carbon 2p states<sup>4,18,19,20</sup>. The phase instability of

stoichiometric YC may be explained based on band filling<sup>20</sup>. In YC, the Fermi level intersects the  $e_g$ -like bands. As a result, the bonding states remain partially unoccupied as distinct for example from the stable B1-ZrC phase, where all bonding states are occupied, whereas antibonding states, on the contrary, are unfilled. The density of states (per formula unit) at the Fermi level  $N(E_F)$  is quite large (Table 1) and comparable with  $N(E_F)$  of B1-NbC. At the same time their compositions are different: for YC the contributions from d and C2p states are comparable (Table 1), while the main role in NbC is played by metallic d states. Note also that inter-atomic bonds and charge distribution in B1-YC are quite isotropic, see Fig. 2. The electronic properties of yttrium dicarbide were studied earlier using the tight-binding linear muffin-tin orbital atomic-sphere approximation (TB-LMTO-ASA) calculations<sup>11,21</sup>. Our FLMTO  $YC_2$  electronic bands and DOSs are shown in Figs. 3, 4 and agree well with those reported in<sup>11,21</sup>. The two lowest bands (Fig. 3) at about 14.4 and 7.1 eV below  $E_F$  are bonding and nonbonding C2s states respectively. The low-lying bonding C2s band with the maximal dispersion of 1.1 eV is separated from the next band group by a gap of about 6.4 eV. The combination of the C2p<sub>x,y</sub> orbitals forms the quasi-flat bands from  $\Gamma$  to Z with the DOS maximum around -4.2 eV, which are hybridized with the Yd<sub>xy</sub> orbitals, Fig. 4. The C2p<sub>z</sub> states split up into two bands (peaks A, B in the partial DOS picture around -7.3 and -2.2 eV) hybridized with the Yd<sub>3z<sup>2</sup>-1</sub> states. All these bands contribute to the Y-C metal bonding and are completely occupied. The partially filled near-Fermi bands (Y4<sub>yz,xz</sub> in the region -2.0 eV  $\div$   $E_F$  and Y4<sub>x<sup>2</sup>-y<sup>2</sup></sub> in the region -0.95 eV  $\div$   $E_F$ ) are strongly dispersive and are hybridized with the antibonding C2p<sub>x,y</sub> orbitals in the direction of axis c. The Fermi level intersects three bands near  $\Gamma$ , P, and Z points. These bands form the Fermi surface, which contains, in particular, hole sheets (around points  $\Gamma$  and Z), Fig. 5. The composition of  $N(E_F)$  includes the contributions from the Yd<sub>xz,yz,x<sup>2</sup>-y<sup>2</sup></sub>, and C2p<sub>x,y</sub> orbitals, see Table 1. The value of the other Yd, C2p components, as well as of the Yp,s and C2s valence states are negligibly small. Thus the electronic structure and the chemical bonding type in yttrium mono- and dicarbide differ essentially: isotropic Y-C bonds in YC versus anisotropic Y-C and C-C bonds in  $YC_2$ , see charge-density contour maps in Fig.2. The calculated bands and DOS for  $Y_2C_3$  are shown in Figs. 6, 7. The valence zone of  $Y_2C_3$  contains four separated band groups (I-IV, Fig. 7). Bands (I) between -14.3 and -13.3 eV are bonding carbon 2s states, whereas antibonding C2s states (with an admixture of C2p<sub>x</sub> and Yd,p,s orbitals) form separate bands (II) in the region -7.1  $\div$  -6.4 eV. The higher completely occupied band group (III) between -5.7 and -2.4 eV comes from Yp,d and C2p orbitals. The Fermi level lies in the middle of bands (IV) composed mostly of Yd-C2p states. The bands intersecting the Fermi level form hole (around H

and N points) and electronic sheets of the Fermi surface. As in  $YC_2$ , the partial DOSs of  $Y_2C_3$  demonstrated very anisotropic orbital states distributions (see also Table 1) depending on the non-equivalency of Y-C and C-C bonds (Fig. 8) and the structural peculiarities of the yttrium sesquicarbide, which contains carbon pairs in different orientations<sup>15</sup>. Of special interest is a near-Fermi DOS  $Y_2C_3$ , since in the conventional BCS-type superconductors the DOS within the interval  $E_F \pm \hbar\Theta_D$  ( $\Theta_D$  - Debye frequency) at the Fermi level is crucial for superconductivity, we show in Fig. 9 the density of states for  $Y_2C_3$  within a small energy interval around  $E_F$ . As is seen from Fig. 9,  $E_F$  is in the region of DOS minimum between two sharp peaks A and B and falls to a local small DOS maximum. Thus, both electronic and hole doping that change the position of  $E_F$  may decrease or increase  $N(E_F)$  and accordingly  $T_c$ . Simple estimations based on the rigid-band model show that  $E_F$  will coincide with maxima A and B, when about 0.7 holes or 0.5 additional electrons are introduced per formula unit of  $Y_2C_3$ . As a result,  $N(E_F)$  of these doped systems increases almost twice (by 89 and 98 % respectively in comparison with  $N(E_F)$  of the stoichiometric yttrium sesquicarbide). This effect may be achieved by several means. The most probable approach is to dope the yttrium sublattice with donor or acceptor

dopants. The role of hole dopants may be played also by carbon vacancies. Another important factor  $N(E_F)$  of the metastable  $Y_2C_3$  phase may be pressure<sup>11,12,13</sup>. The immediate prospects of our studies will involve simulation of pressure effects on fine peculiarities of the electronic band structure of  $Y_2C_3$ . In summary, our FLMTD calculations of the electronic band structure of the bcc yttrium sesquicarbide indicate that the enhanced transition temperature as compared with  $YC_2$  may be due to electronic factors: the DOS at the Fermi level for  $Y_2C_3$  was found to be about 40 % higher than that for 4-K SC  $YC_2$ , Table 1. In addition, the contribution from the C2p states increases appreciably. Since the Fermi level of the "ideal" stoichiometric bcc yttrium sesquicarbide is located near the local DOS minimum, the superconducting properties of  $Y_2C_3$ -based materials will be very sensitive to synthesis conditions (for example, pressure and annealing effects) and the presence of lattice defects. By changing these factors it is possible to vary the  $T_c$  of the Y-C phase in a wide range.

#### Acknowledgment.

This work was supported by the RFBR, grant 02-03-32971, and the Russian Foundation for Scientific Schools, grant SS 829.2003.3.

- 
- <sup>1</sup> L. E. Toth, Transition Metal Carbides and Nitrides, Academic Press, New York, 1971.
- <sup>2</sup> S. V. Vonsovsky, Yu. A. Izumov, E. Z. Kurmaev, Superconductivity in Transition Metals, their Alloys and Compounds. Springer-Verlag, Berlin, 1982.
- <sup>3</sup> C. P. Poople, Jr., Y. A. Farach, J. Supercond. **13** (2000) 47.
- <sup>4</sup> G. L. W. Hart, B. M. Klein, Phys. Rev. **B61** (2000) 3151.
- <sup>5</sup> R. W. Henn, W. Schnelle, R. K. Kremer, A. Simon, Phys. Rev. Lett. **77** (1996) 374.
- <sup>6</sup> R. J. Cava, H. Takagi, B. Batlogg, H. W. Zandbergen, J. J. Krajewski, W. F. Peck, Jr., R. B. van Dover, R. J. Felder, T. Siegrist, K. Mizushashi, J. O. Lee, H. Eisaki, S. A. Carter, S. Uchida, Nature (London) **367** (1994) 146.
- <sup>7</sup> R. J. Cava, H. Takagi, H. W. Zandbergen, J. J. Krajewski, W. F. Peck, Jr., T. Siegrist, B. Batlogg, R. B. van Dover, R. J. Felder, K. Mizuhashi, J. O. Lee, H. Eisaki, S. Uchida, Nature (London) **367** (1994) 252.
- <sup>8</sup> A.L. Ivanovskii, Russ. Chem. Rev. **67** 403 (2001).
- <sup>9</sup> S. N. Behera, B. N. Panda, G. C. Rout, P. Entel, Int. J. Modern Phys. **B15** (2001) 2519.
- <sup>10</sup> I. S. Yang, M. V. Klein, S. Bud'ko, P. C. Canfield, J. Phys. Chem. Solids. **63** (2002) 2195.
- <sup>11</sup> Th. Gulden, R. W. Henn, O. Jepsen, R. K. Kremer, W. Schnelle, A. Simon, C. Felser, Phys. Rev. **B56** (1997) 9021.
- <sup>12</sup> G. Amano, S. Akutagawa, T. Muranaka, Y. Zenitani, J. Akimitsu, cond-mat/0311517 (2003).
- <sup>13</sup> M.C. Krupka, A.L. Giorgi, N.H. Krikorian, E.G. Szklarz, J. Less-Common Metals **17** (1969) 91.
- <sup>14</sup> T. Nakane, T. Mochiku, H. Kito, M. Nagao, J. Itoh, H. Kumakura, Y. Takano, cond-mat/0311561 (2003).
- <sup>15</sup> V. I. Novokshonov, Russ. J. Inorgan. Chem. **25** (1980) 375.
- <sup>16</sup> S.Y. Savrasov, Phys. Rev. **B54** (1996) 16470.
- <sup>17</sup> J.P. Perdew, K. Burke, M. Ernzerhof, Phys. Rev. Lett. **77** (1996) 3865.
- <sup>18</sup> A. Neckel, P. Rastl, R. Eibler et al., J. Phys. C: Solid State Phys. **9** (1976) 759.
- <sup>19</sup> P. Marksteiner, P. Weinberger, A. Neckel, R. Zeller, P. H. Dederichs, Phys. Rev. **B33** (1986) 812.
- <sup>20</sup> V. A. Gubanov, A. L. Ivanovskii, V.P. Zhukov. Electronic Structure of Refractory Carbides and Nitrides, University Press, Cambridge, 1994.
- <sup>21</sup> V. P. Zhukov, D.L. Novikov, N.I. Medvedeva, V. A. Gubanov, J. Struct. Chem. **30** (1989) 553.

TABLE I: . Total and site-projected  $\ell$ -decomposed DOSs at the Fermi level ( $N(E_F)$ , states/eV).

Density of state Partial states on atom Total state on molecule	YC	YC <sub>1.5</sub>	YC <sub>2</sub>
<b>C2s</b>	0,0088	0,0076	0,0104
C2p <sub>x</sub>	0,3849	0,1856	0,0501
C2p <sub>y</sub>	0,3849	0,0293	0,0501
C2p <sub>z</sub>	0,3849	0,0937	0,0089
<b>C2p</b>	1,1546	0,3086	0,1091
<b>Ys</b>	0,0084	0,0260	0,0039
Yp <sub>x</sub>	0,0221	0,0153	0,0004
Yp <sub>y</sub>	0,0221	0,0153	0,0004
Yp <sub>z</sub>	0,0221	0,0153	0,0004
<b>Yp</b>	0,0664	0,0459	0,0011
Yd <sub>yz</sub>	0,0918	0,0843	0,2048
Yd <sub>xz</sub>	0,0918	0,0843	0,2048
Yd <sub>xy</sub>	0,0918	0,08432	0,0060
Yd <sub>x<sup>2</sup>-y<sup>2</sup></sub>	0,1064	0,2059	0,1036
Yd <sub>3z<sup>2</sup>-1</sub>	0,1064	0,2059	0,0025
<b>Yd</b>	0,4882	0,6647	0,5217
<b>Total</b>	1.7265	1.2107	0.7658

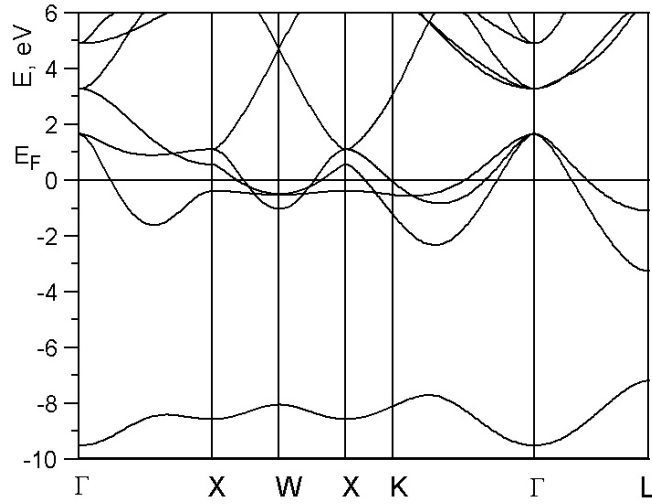


FIG. 1: The band structure of hypothetical B1-YC.

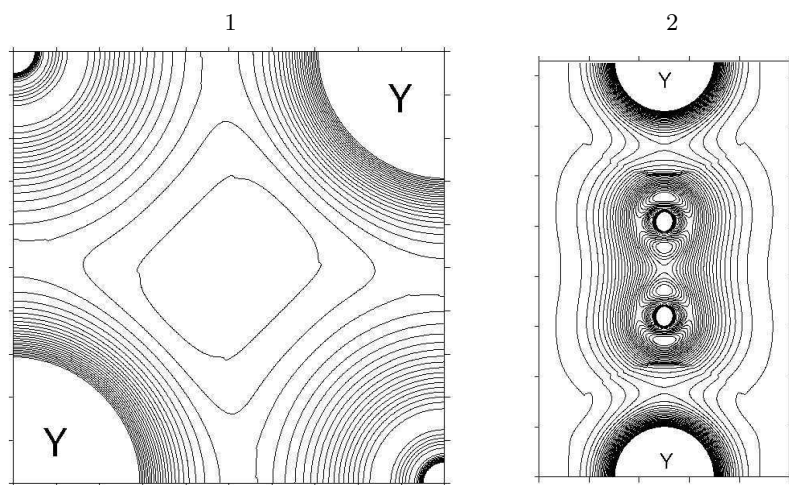


FIG. 2: Constant charge-density contour maps in sections of yttrium mono- (1) - and dicarbide (2) cells illustrating the formation of isotropic Y-C and anisotropic C-C bonds respectively.

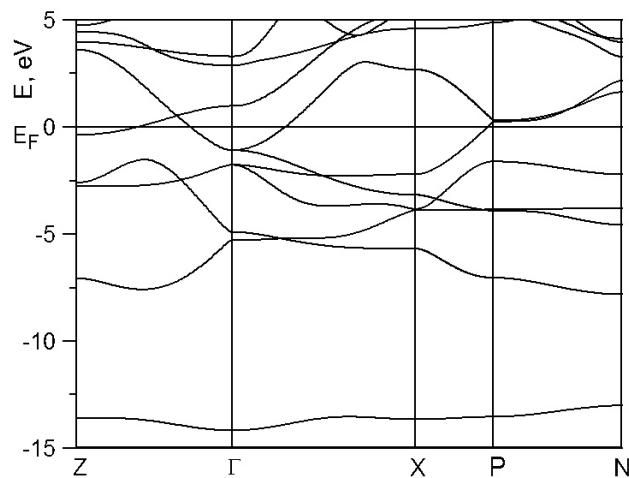


FIG. 3: The band structure of YC<sub>2</sub>.

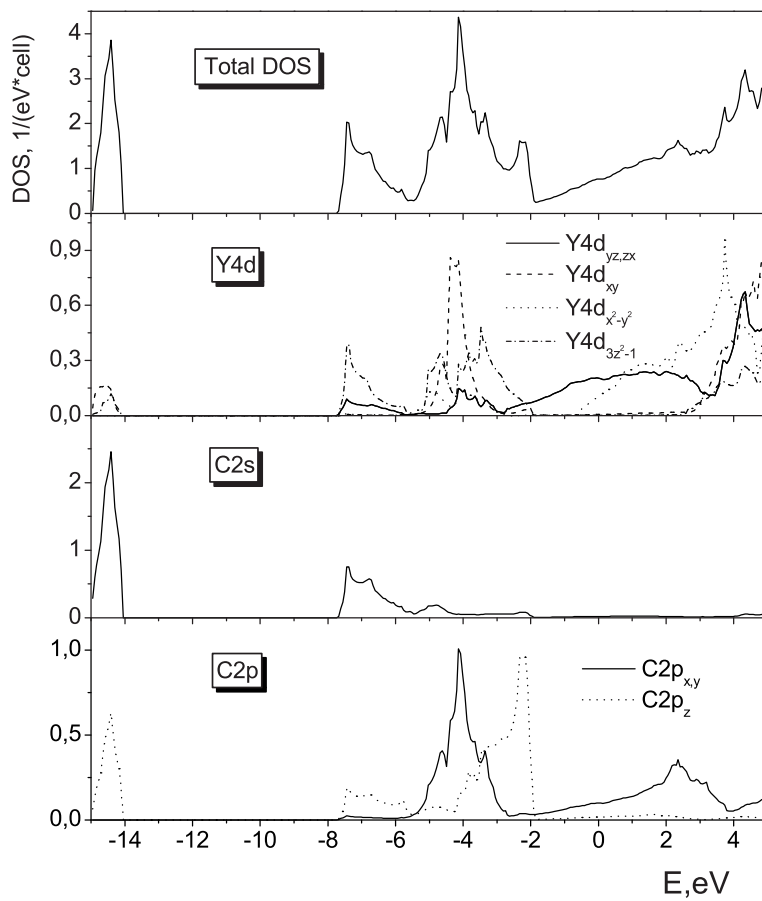


FIG. 4: The total and partial densities of states for  $YC_2$ .

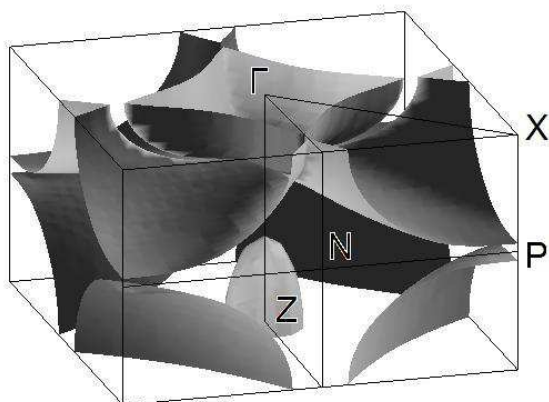


FIG. 5: The Fermi surface for  $YC_2$ .

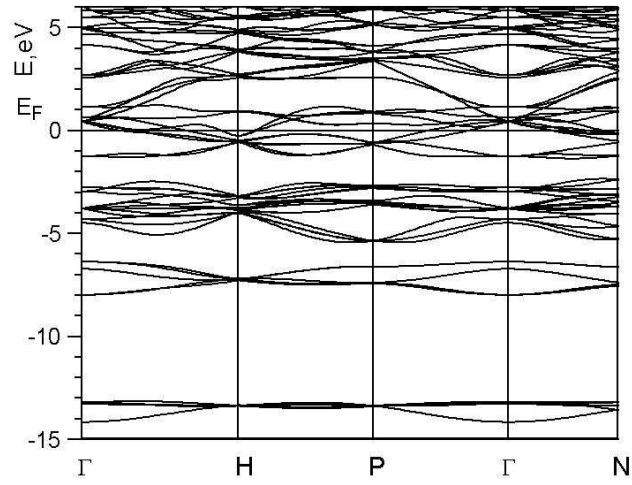


FIG. 6: The band structure of  $Y_2C_3$  calculated with the lattice constants as given in Ref.<sup>15</sup> using the full-potential LMTO method.

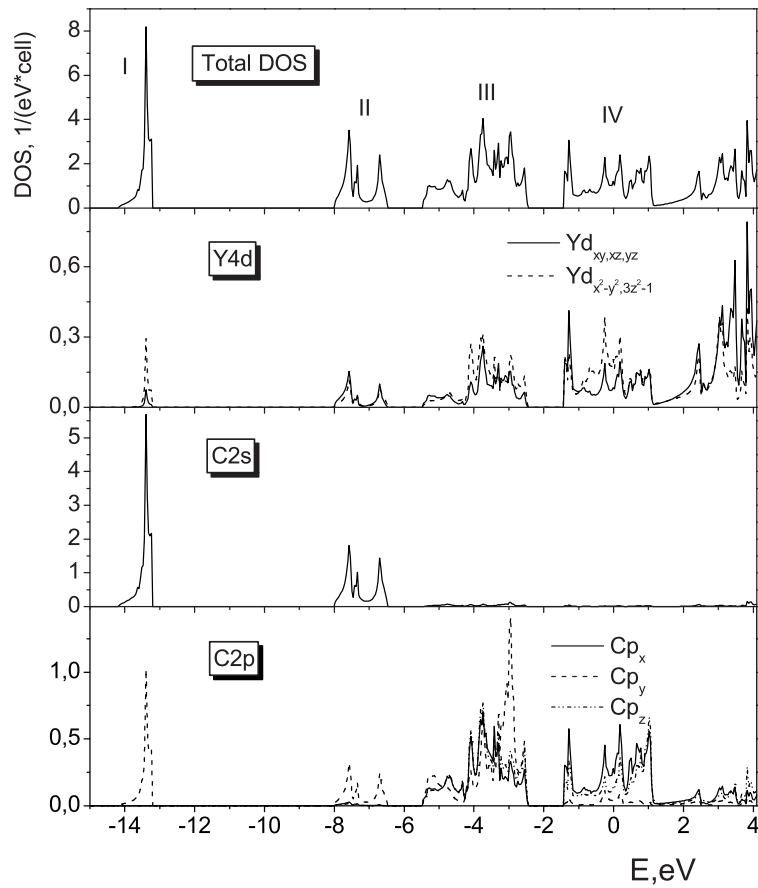


FIG. 7: The total and partial DOSs for  $Y_2C_3$  calculated with the lattice constants as given in Ref.<sup>15</sup> using the full-potential LMTO method.

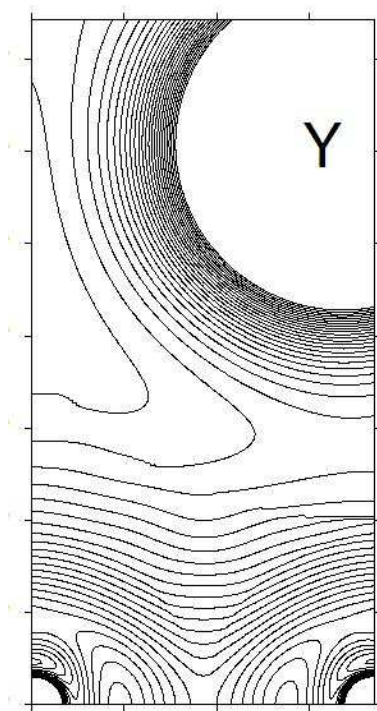


FIG. 8: The charge density map in the section of  $Y_2C_3$  cell illustrating the C-C covalent bond.

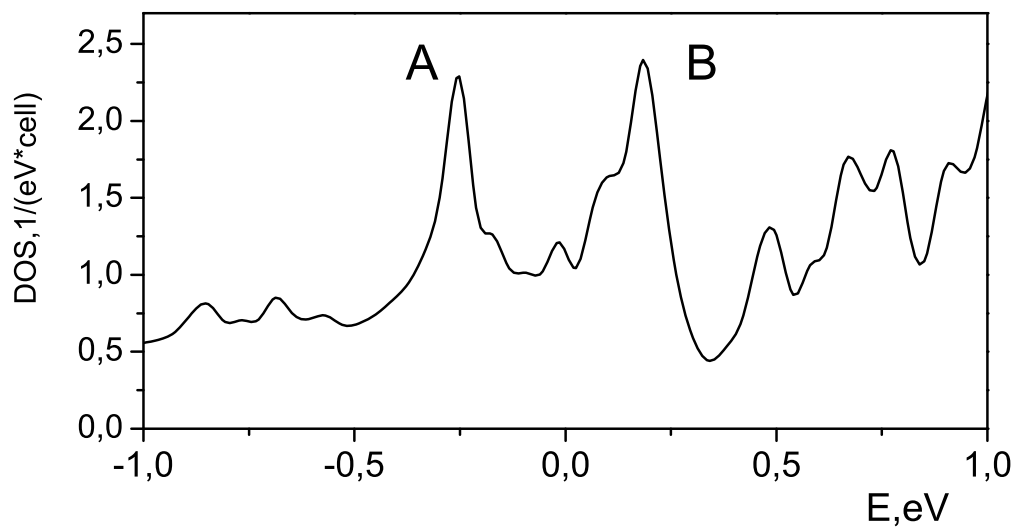


FIG. 9: The total density of states of  $Y_2C_3$  around the Fermi energy calculated with the lattice constants as given in Ref.<sup>15</sup>.